LETTERS
PUBLISHED ONLINE: 31 OCTOBER 2010 | DOI: 10.1038/NNANO.2010.212
nature nanotechnology

Nanomechanical recognition measurements of individual DNA molecules reveal epigenetic methylation patterns

Rong Zhu[1,2], Stefan Howorka[3,4], Johannes Pröll[5†], Ferry Kienberger[1], Johannes Preiner[1], Jan Hesse[1,3], Andreas Ebner[1], Vassili Ph. Pastushenko[1], Hermann J. Gruber[1] and Peter Hinterdorfer[1,2,3*]

Atomic force microscopy[1] (AFM) is a powerful tool for analysing the shapes of individual molecules and the forces acting on them. AFM-based force spectroscopy provides insights into the structural and energetic dynamics[2–4] of biomolecules by probing the interactions within individual molecules[5,6], or between a surface-bound molecule and a cantilever that carries a complementary binding partner[7–9]. Here, we show that an AFM cantilever with an antibody tether can measure the distances between 5-methylcytidine bases in individual DNA strands with a resolution of 4 Å, thereby revealing the DNA methylation pattern, which has an important role in the epigenetic control of gene expression. The antibody is able to bind two 5-methylcytidine bases of a surface-immobilized DNA strand, and retracting the cantilever results in a unique rupture signature reflecting the spacing between two tagged bases. This nanomechanical approach might also allow related chemical patterns to be retrieved from biopolymers at the single-molecule level.

Reading DNA sequences in a single-molecule[10–12] and label-free[13–15] fashion remains a challenge in modern biology. Direct mechanical measurements on nucleic acids[16] have revealed the sequence-specific mechanism of DNA unzipping[17–19] and RNA unfolding[20]. However, thermal fluctuations and the weakness of the base-pair interactions have limited the resolution of this approach to ten base pairs[21], which is insufficient to read individual separate bases along an individual DNA strand. A specific challenge is to understand 5-methylcytosine-carrying DNA sequences that play a crucial role in epigenetic gene regulation, but are difficult to read with conventional ensemble methods[22,23], especially when 5-hydroxymethylcytosine[24] is involved.

We have developed an atomic force microscope (AFM)-based nanomechanical approach that measures the distance between 5-methylcytosine bases in individual DNA strands and thereby determines the methylation pattern. The experimental components and principle of the approach are shown schematically in Fig. 1a. A monoclonal antibody specific for 5-methylcytidine is conjugated[25] via a flexible poly(ethylene glycol) (PEG) crosslinker to an AFM cantilever tip, and a 5-methylcytidine-containing single-stranded DNA (ssDNA) oligonucleotide is coupled via its 3′-terminus to a glass slide[26]. Bringing the AFM tip into contact with the slide surface leads to the formation of two molecular bonds between the Fab arms of the antibody and two methylcytosine bases on the ssDNA (Fig. 1a, panel 1). Retracting the cantilever first elongates the flexible PEG and a section of the DNA strands (Fig. 1a, panel 2), and then sequentially breaks the first and second bonds (Fig. 1a, panels 3 and 4, respectively). These molecular changes are reflected in the corresponding force–distance curve (Fig. 1b), as indicated by the gradual increase in force (Fig. 1b, part 1 of the curve). Importantly, the rupture of the two base-mediated bonds leads to two unique peaks in the force–distance curve (Fig. 1b, parts 2 and 3 of the curve), revealing the exact distance between the bases in the DNA strand.

The approach to measuring molecular dimensions by means of rupture distances was experimentally validated with ssDNA

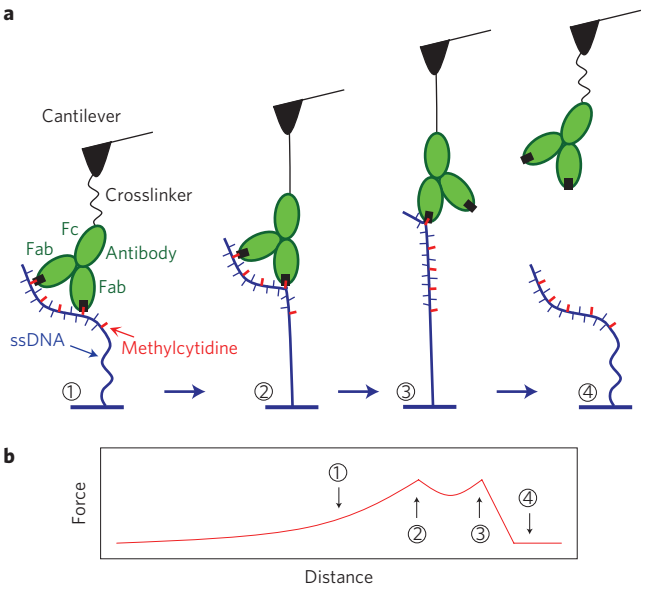

Figure 1 | A single-molecule force spectroscopy experiment reveals the molecular distance between two 5-methylcytosine bases in a DNA strand. **a**, ssDNA is coupled to an aldehyde-bearing glass surface through an amine group at its 3′-end, and the antibody is tethered via a lysine residue or its natural oligosaccharide and a flexible PEG crosslinker to the cantilever tip. The two Fab-arms and the Fc-arm of the antibody are indicated. Panels 1, 2, 3 and 4 correspond to different states that occur upon retracting the cantilever from the surface, including the elongation of the PEG and DNA strands and the sequential breaking of the two methylcytosine antibody bonds. **b**, These molecular changes are reflected in a force–distance curve, with the rupture distance in the curve (points 2 to 3) corresponding to the spacing between two 5-methylcytidines in a DNA strand.

[1]Institute for Biophysics, Johannes Kepler University of Linz, A-4040 Linz, Austria, [2]Christian Doppler Laboratory for Nanoscopic Methods in Biophysics, Johannes Kepler University of Linz, A-4040 Linz, Austria, [3]Center for Advanced Bioanalysis GmbH, 4020 Linz, Austria, [4]University College London, Department of Chemistry, London WC1H 0AJ, UK, [5]Department of Internal Medicine I, Elisabethinen Hospital, A-4010 Linz, Austria; [†]Present address: Red Cross Transfusion Service of Upper Austria, A-4020 Linz, Austria.*e-mail: peter.hinterdorfer@jku.at

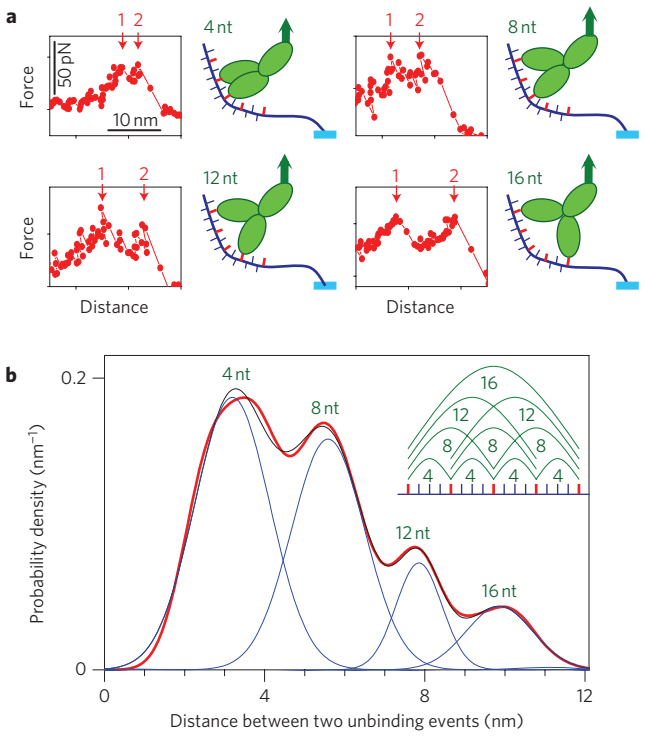

Figure 2 | A two-step unbinding event between antibody and methylcytosine-containing ssDNA. a, Examples of antibody–DNA ruptures with two unbinding events (indicated by red arrows, 1 and 2). The sketches show the possible binding positions of the antibody on the DNA, with 4, 8, 12 and 16 nucleotides (nt) separation. **b**, Distribution of the distances between two unbinding events. The thick red line represents the experimental probability density function of distances constructed from distance values of 224 force curves. The thin lines are the result of a multiple Gaussian fit. Inset: possible pairs of dual antibody binding.

carrying 5-methylcytosine bases separated by three nucleotides each. Representative force–distance curves featured two-step rupture signatures with spacings of 4, 8, 12 and 16 nucleotides between the methylcytosine bases (Fig. 2a), in line with expectations for the sequential breaking of the molecular bonds with two methylcytosine bases. The measurements also revealed single-step traces that stem from DNA strands bound by a single Fab arm (Supplementary Fig. S1). Over 200 dual-rupture curves were combined to obtain a probability density distribution (red line in Fig. 2b) for quantitative analysis using multiple Gaussian fitting (blue lines in Fig. 2b). The four quasi-equidistant peaks in the distribution feature peak maxima and widths (3.2 ± 0.94 nm, 5.6 ± 0.92 nm, 7.9 ± 0.57 nm and 9.9 ± 0.84 nm) that correspond well to the four different nucleotide distances between various pairs from the total pool of five 5-methylcytidines. The derived normalized average distance per nucleotide of 0.62–0.70 nm, obtained for spacings of 8, 12 and 16 nucleotides, was indeed in very good agreement with the theoretical value of 0.59 nm for the C3-endo and 0.70 nm for the C2-endo conformation of the ribose unit in the DNA backbone[16]. Similar calculations for a spacing of four nucleotides yielded a slightly greater normalized distance per nucleotide, which might be caused by mechanical twists or kinks of the Fab-arms upon binding, due to the enforced short distance between the two 5-methylcytidines (2.4–2.8 nm in stretched configuration, compared to the intrinsic antibody thickness of 3.5 nm). Further analysis of the probability density distribution revealed that the height of the peaks related to the probability of the occurrence of two-step unbinding events, was consistent with the number of possible combinations for the molecular interactions between two Fab arms and the five 5-methylcytosine bases. According to simple theoretical considerations (Fig. 2b, inset), the spatial distances of 4, 8, 12 and 16 nucleotides should occur 4, 3, 2 and 1 times, respectively. The relative peak heights in the distribution of Fig. 2b consistently corresponded to the approximate ratio of 4/3/2/1. These findings strongly indicate independent binding of the two Fab-arms (that is, lack of cooperativity[27]), which must be due to the high overall flexibility of the antibody domains[28] and the DNA[16]. Both antibody and DNA act as highly dynamic molecular calipers capable of screening and gauging distances on the nanoscale, made possible by their ability to adopt a vast number of conformations.

The method was further tested using another DNA sample containing nine 5-methylcytidines separated by six nucleotides to confirm that discrete AFM signatures can be obtained (Fig. 3a). The experimental probability density distribution of the rupture distances revealed six distinct peaks (Fig. 3b). Their maxima were located at 3.9 ± 1.10 nm, 7.5 ± 1.17 nm, 10.9 ± 1.06 nm, 14.7 ± 0.82 nm, 17.8 ± 0.73 nm and 21.4 ± 0.60 nm, respectively, and correlated well with the distances between two 5-methylcytidines separated

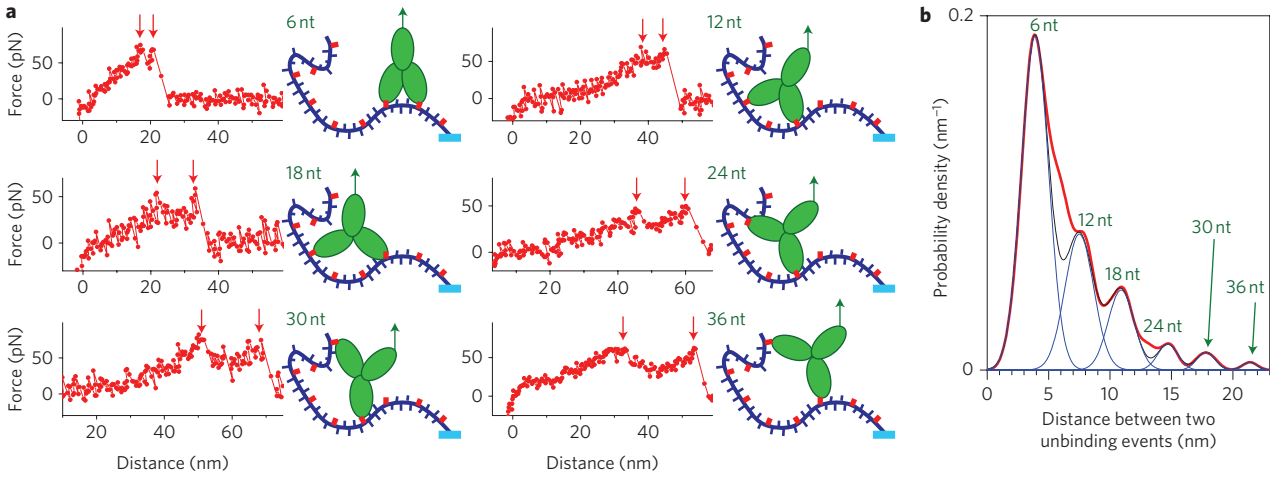

Figure 3 | Two-step unbinding from ssDNA with nine 5-methylcytidines separated by six nucleotides. a, Examples of force–distance curves with sketches showing the possible binding positions of the antibody on the DNA. **b**, Distribution of the rupture distance between two unbinding events. The thick red line represents the experimental probability density function of distances constructed from 150 force curves. The thin lines are the result of a multiple Gaussian fit.

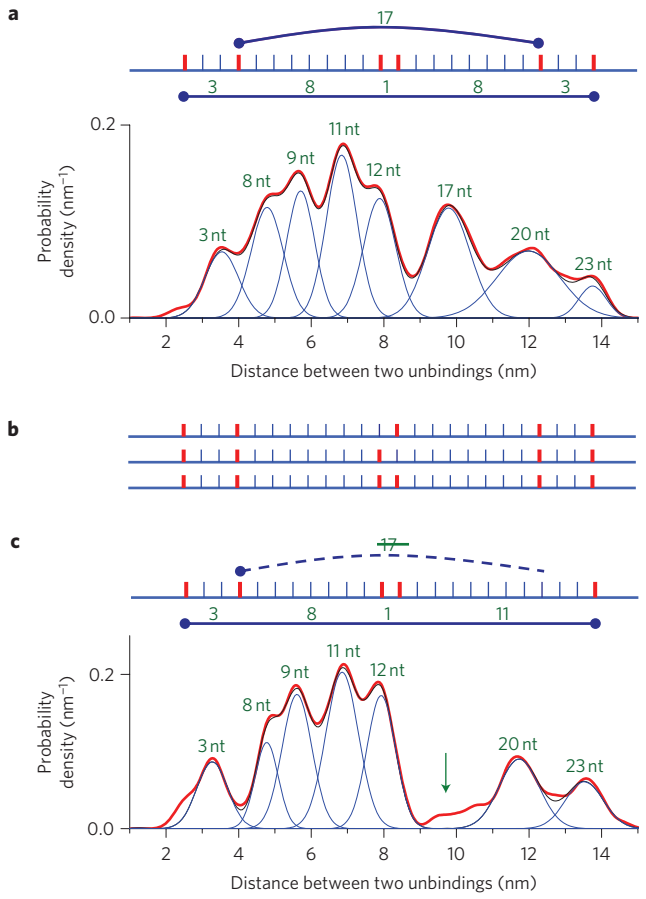

Figure 4 | Single nucleotide resolution enables 5-methylcytidine sequencing and the detection of single epigenetic changes. a, Distance distribution from a DNA containing six 5-methylcytidines separated by 3, 8, 1, 8 and 3 nucleotides. The thick red line represents the experimental probability density function of distances constructed from distance values of 298 force curves. The thin lines are the result of a multiple Gaussian fit. **b**, Three possible sequences can be reconstructed (see text for explanation) from the peaks corresponding to 3, 8, 9, 11, 12, 17, 20 and 23 nucleotides in the distance distribution in **a**. **c**, Removal of a single methyl group from the DNA. The distance distribution shows similar peaks when compared to those in **a**, except for the absence of the peak corresponding to 17 nucleotides. The thick red line represents the experimental probability density function of distances constructed from distance values of 216 force curves. The thin lines are the result of a multiple Gaussian fit.

by 6, 12, 18, 24, 30 and 36 nucleotides, respectively (average length of 0.59–0.65 nm per nucleotide). The peaks with the two longest possible rupture distances (corresponding to 5-methylcytosine separated by 42 and 48 nucleotides) were not observed, most probably due to the decreasing number of possible combinations for reaching longer distances on the ssDNA.

To inspect whether the single-molecule approach can infer sequence information with single-base resolution, we attached the antibody to the cantilever via one of the two natural oligosaccharide chains located in the hinge region between the Fab and Fc arms. In contrast to the above used random and non-directed lysine-based coupling method, the oligosaccharide-based procedure is site-specific and therefore aligns the tip-bound antibody along the pulling axis and improves the resolution in the rupture distance measurements. The optimized antibody cantilever was used to examine DNA strands with six 5-methylcytidines separated by 3, 8, 1, 8 and 3 nucleotides (Fig. 4a). Possible rupture distances for this pattern are 1, 3, 8, 9, 11, 12, 17, 20 and 23 nucleotides. The experimental distribution of distances between two unbinding events were in agreement with the peaks (Fig. 4a), which corresponds to lengths of 8, 9, 11, 12, 17, 20 and 23 nucleotides, respectively (peak maxima at 4.8 ± 0.44 nm, 5.7 ± 0.39 nm, 6.8 ± 0.42 nm, 7.9 ± 0.44 nm, 9.9 ± 0.58 nm, 12.0 ± 0.87 nm and 13.8 ± 0.37 nm; average nucleotide length, 0.58–0.66 nm). The first peak correlated to a distance of three nucleotides, but had a slightly larger length interval (3.5 ± 0.46 nm), consistent with the position of the first peak in Fig. 2b. The two neighbouring 5-methylcytidines could not be bound by one antibody, or at least its unbinding steps were not discernible. Importantly, a distance of 8 nucleotides could be clearly distinguished from 9, and 11 could be discerned from 12, with a resolution of about 4 Å, as determined by the width of single Gaussians fits.

After demonstrating that a given methylcytosine pattern yields a unique distribution of rupture distances, we probed whether the opposite is also true, that is, whether a given distribution encodes for a distinct methylation pattern. We tested this possibility by re-examining the rupture data from the previous experiment (Fig. 4a). Without *a priori* knowledge, the distribution pattern with 5-methylcytidine distances of 3, 8, 9, 11, 12, 17, 20 and 23 nucleotides (Fig. 4a) was used as the experimental input to derive three possible methylation patterns (Fig. 4b). They show almost identical features and differ by the presence and position of only one 5-methylcytidine (Fig. 4b).

We finally examined whether our single-molecule method is capable of detecting single-nucleotide epigenetic changes. For this purpose, we selected a sequence of a previously examined strand (Fig. 4a), but substituted cytidine for 5-methylcytidine at position 20. The corresponding distribution of rupture distances (Fig. 4c, peak maxima at 3.3 ± 0.42 nm, 4.8 ± 0.32 nm, 5.6 ± 0.41 nm, 6.9 ± 0.45 nm, 7.9 ± 0.39 nm, 11.7 ± 0.55 nm and 13.5 ± 0.52 nm; average nucleotide length 0.59–0.66 nm) shows a similar pattern to the strand with the 5-methylcytidine in position 20 (Fig. 4a). However, the peak corresponding to an interval of 17 nucleotides (the distance between 5-methylcytidines on positions 3 and 20) was missing. Therefore, the substitution of one single methyl group was unequivocally verified.

This study presents a single-molecule method for the analysis of biologically relevant methylation sequences of short ssDNA strands with single-nucleotide resolution. Antibodies were used as molecular bivalent calipers and demonstrated remarkable dynamic, nanomechanical and specific-binding capabilities. The sensing of bases separated by very short or very long distances may be further improved using artificial multivalent calipers composed of flexibly joined small antibody fragments[29] or antibody-like molecules[30,31].

With further experimentation, our single-molecule sensing method can be readily applied to biological samples by using short genomic ssDNA fragments hybridized to oligonucleotide microarrays[32]. The approach is also compatible with cantilever arrays for parallel high-throughput measurements of DNA chips and may be extended to sense other bases and base analogues[33]. By mapping the distance of chemical tags within individual biomolecules at subnanoscale resolution, the nanomechanical strategy may have the potential to directly retrieve related biochemical information from other biopolymers such as post-transcriptionally modified polypeptides.

Received 31 March 2010; accepted 1 October 2010;
published online 31 October 2010

References

1. Binnig, G., Quate, C. F. & Gerber, C. Atomic force microscope. *Phys. Rev. Lett.* **56,** 930–933 (1986).
2. Merkel, R., Nassoy, P., Leung, A., Ritchie, K. & Evans, E. Energy landscapes of receptor–ligand bonds explored with dynamic force spectroscopy. *Nature* **397,** 50–53 (1999).

3. Baumgartner, W. *et al.* Cadherin interaction probed by atomic force microscopy. *Proc. Natl Acad. Sci. USA* **97,** 4005–4010 (2000).
4. Oesterhelt, F. *et al.* Unfolding pathways of individual bacteriorhodopsins. *Science* **288,** 143–146 (2000).
5. Rief, M., Oesterhelt, F., Heymann, B. & Gaub, H. E. Single molecule force spectroscopy on polysaccharides by atomic force microscopy. *Science* **275,** 1295–1297 (1997).
6. Oberhauser, A. F., Marszalek, P. E., Erickson, H. P. & Fernandez, J. M. The molecular elasticity of the extracellular matrix protein tenascin. *Nature* **393,** 181–185 (1998).
7. Lee, G. U., Chrisey, L. A. & Colton, R. J. Direct measurement of the forces between complementary strands of DNA. *Science* **266,** 771–773 (1994).
8. Moy, V. T., Florin, E. L. & Gaub, H. E. Intermolecular forces and energies between ligands and receptors. *Science* **266,** 257–259 (1994).
9. Hinterdorfer, P., Baumgartner, W., Gruber, H. J., Schilcher, K. & Schindler, H. Detection and localization of individual antibody–antigen recognition events by atomic force microscopy. *Proc. Natl Acad. Sci. USA* **93,** 3477–3481 (1996).
10. Braslavsky, I., Hebert, B., Kartalov, E. & Quake, S. R. Sequence information can be obtained from single DNA molecules. *Proc. Natl Acad. Sci. USA* **100,** 3960–3964 (2003).
11. Greenleaf, W. J. & Block, S. M. Single-molecule, motion-based DNA sequencing using RNA polymerase. *Science* **313,** 801 (2006).
12. Eid, J. *et al.* Real-time DNA sequencing from single polymerase molecules. *Science* **323,** 133–138 (2009).
13. Branton, D. *et al.* The potential and challenges of nanopore sequencing. *Nature Biotechnol.* **26,** 1146–1153 (2008).
14. Clarke, J. *et al.* Continuous base identification for single-molecule nanopore DNA sequencing. *Nature Nanotech.* **4,** 265–270 (2009).
15. Chang, S. *et al.* Tunnelling readout of hydrogen-bonding-based recognition. *Nature Nanotech.* **4,** 297–301 (2009)
16. Smith, S. B., Cui, Y. & Bustamante, C. Overstretching B-DNA: the elastic response of individual double-stranded and single-stranded DNA molecules. *Science* **271,** 795–799 (1996).
17. Essevaz-Roulet, B., Bockelmann, U. & Heslot, F. Mechanical separation of the complementary strands of DNA. *Proc. Natl Acad. Sci. USA* **94,** 11935–11940 (1997).
18. Rief, M., Clausen-Schaumann, H. & Gaub, H. E. Sequence-dependent mechanics of single DNA molecules. *Nat. Struct. Biol.* **6,** 346–349 (1999).
19. Krautbauer, R., Rief, M. & Gaub, H. E. Unzipping DNA oligomers. *Nano Lett.* **3,** 493–496 (2003).
20. Liphardt, J., Onoa, B., Smith, S. B., Tinoco, I. J. & Bustamante, C. Reversible unfolding of single RNA molecules by mechanical force. *Science* **292,** 733–737 (2001).
21. Voulgarakis, N. K., Redondo, A., Bishop, A. R. & Rasmussen, K. O. Sequencing DNA by dynamic force spectroscopy: limitations and prospects. *Nano Lett.* **6,** 1483–1486 (2006).
22. Frommer, M. *et al.* A genomic sequencing protocol that yields a positive display of 5-methylcytosine residues in individual DNA strands. *Proc. Natl Acad. Sci. USA* **89,** 1827–1831 (1992).
23. Rein, T., DePamphilis, M. L. & Zorbas, H. Identifying 5-methylcytosine and related modifications in DNA genomes. *Nucleic Acids Res.* **26,** 2255–2264 (1998).
24. Huang, Y. *et al.* The behaviour of 5-hydroxymethylcytosine in bisulfite sequencing. *PLoS One* **5,** e8888 (2010)
25. Ebner, A. *et al.* A new, simple method for linking of antibodies to atomic force microscopy tips. *Bioconjug. Chem.* **18,** 1176–1184 (2007).
26. Schlapak, R. *et al.* Glass surfaces grafted with high-density poly(ethylene glycol) as substrates for DNA oligonucleotide microarrays. *Langmuir* **22,** 277–285 (2006).
27. Kienberger, F., Mueller, H., Pastushenko, V. & Hinterdorfer, P. Following single antibody binding to purple membranes in real time. *EMBO Rep.* **5,** 579–583 (2004).
28. Saphire, E. O. *et al.* Contrasting IgG structures reveal extreme asymmetry and flexibility. *J. Mol. Biol.* **319,** 9–18 (2002).
29. Hamers-Casterman, C. *et al.* Naturally occurring antibodies devoid of light chains. *Nature* **363,** 446–448 (1993).
30. Kohl, A. *et al.* Designed to be stable: Crystal structure of a consensus ankyrin repeat protein. *Proc. Natl Acad. Sci. USA* **100,** 1700–1705 (2003).
31. Schneider, G. & Fechner, U. Computer-based de novo design of drug-like molecules. *Nat. Rev. Drug. Discov.* **4,** 649–663 (2005).
32. Pröll, J. *et al.* Ultra-sensitive immunodetection of 5′-methyl cytosine for DNA methylation analysis on oligonucleotide microarrays. *DNA Res.* **13,** 37–42 (2006).
33. Erlanger, B. F. & Beiser, S. M. Antibodies specific for ribonucleosides and ribonucleotides and their reaction with DNA. *Proc. Natl Acad. Sci. USA* **52,** 68–74 (1964).

Acknowledgements

The authors thank L. Wildling, R. Schlapak, C. Riese, C. Hesch, J. Jacak and C. Rankl for expert technical assistance, and G. Kada, G. Schütz, D. Blaas, A. Frischauf and C. Aberger for enlightening discussions. This work was supported by the Gen-Au project 'Ultra sensitive Proteomics and Genomics' from the Austrian federal ministry for education, science and culture (R.Z., S.H., J.Pröll, P.H.), the Austrian science fund project P15295 (H.J.G.), the Austria Nano-Initiative/NABIOS (R.Z., S.H., H.J.G., P.H.), the European Commission grant 'Single Molecule Workstation (SMW)' no. NMP4-SE-2008-213717 (R.Z., F.K., P.H.), and the Austrian Science Fund project L422-N20 (J.H.).

Author contributions

R.Z. performed the experiments and data evaluation. S.H. developed the surface chemistry and co-wrote the paper. J.Pröll performed the surface chemistry and selected the DNA sequences. F.K., J.Preiner and A.E. discussed the results. J.H. contributed to the surface chemistry. V.Ph.P. programmed the data evaluation. H.J.G. developed the tip chemistry. P.H. led the experimental design and wrote the paper.

Additional information

The authors declare no competing financial interests. Supplementary information accompanies this paper at www.nature.com/naturenanotechnology. Reprints and permission information is available online at http://npg.nature.com/reprintsandpermissions/. Correspondence and requests for materials should be addressed to P.H.